ELSEVIER

Polymer 40 (1999) 6023–6029

polymer

Effects of graphite content on the morphology and barrier properties of poly(vinylidene fluoride) composites

Deanna N. Busick[1], Richard J. Spontak, C. Maurice Balik*

Department of Materials Science and Engineering, Box 7907, North Carolina State University, Raleigh, NC 27695-7907, USA

Received 4 August 1998; received in revised form 1 November 1998; accepted 17 November 1998

Abstract

We have performed a series of morphology and CO_2-probe diffusion analyses to ascertain the existence and composition dependence of voids in graphite/poly(vinylidene fluoride) composites both above and below the graphite percolation threshold, as determined from electrical conductivity measurements. Sorption data indicate that, with increasing graphite loading: (i) the diffusivity of CO_2 in the composite material decreases; and (ii) the volume fraction of voids in the material increases. Differential scanning calorimetry reveals that polymer crystals nucleate heterogeneously on graphite particles and that samples containing graphite have higher degrees of crystallinity than the neat polymer. Crystallinity effects appear to dominate barrier properties at low graphite loadings, while porosity effects dominate at high graphite loadings. Our results strongly suggest that, although voids in these composites are probably associated with relatively poor adhesion along graphite/polymer interfaces, the voids are also discrete (i.e. they do not form a continuous network, even if the graphite particles do).

Keywords: Diffusion; Graphite; Poly(vinylidene fluoride)

1. Introduction

1.1. Background

Polymer/graphite composites have long been employed in structural, aerospace and sporting goods applications. In recent years, increasing attention has been devoted to developing graphite/polymer composites for applications where electrical conductivity is required [1–4]. In addition to high electrical conductivities, these so-called conductive polymer composites (CPCs) often possess other desirable properties, such as corrosion resistance, low cost and ease of processing. Given this combination of properties, graphite/polymer composites present an attractive alternative to metal conductors in certain applications, provided that sufficient electrical conductivity can be achieved.

Electrical conductivity in graphite/polymer composites can only be attained when a connected (percolated) network of graphite particles is present. For any given graphite/polymer system, the graphite percolation threshold, p_c, is the critical concentration of graphite particles which results in the formation of such a network, also called an infinite cluster, and thus the ability to carry electric current. As such, measurements of electrical conductivity are widely used to determine the percolation thresholds of graphite in various polymer matrices [3–7]. According to percolation theory, the electrical conductivity, $\sum$, of a sample is related to the concentration, p, of conductive particles by:

$$\sum \propto (p - p_c)^{\mu} \tag{1}$$

where $\mu = 2$ for a three-dimensional system ($d = 3$) [8].

While the electrical conduction and percolation behavior of graphite in polymer matrices is generally well understood, to date few analyses of the effect of the presence or amount of graphite on the barrier properties of these materials have been reported. However, the barrier properties of a CPC can significantly affect its performance in an intended application. Most applications of CPCs require high electrical conductivity, low permeability to liquids or vapors, and good corrosion resistance. All of these desired properties can be significantly compromised by the presence of pores or voids in the material. Some diffusion and permeation of small molecules through the polymer component of the composite is to be expected, but the presence of voids can drastically increase the material's permeability and

* Corresponding author. Tel.: + (919)-515-2126; fax: + (919)-515-7724.

E-mail address: balik@ncsu.edu (C.M. Balik)

[1] Current address: Materials Science and Technology Division, MS D429, Los Alamos National Laboratory, Los Alamos, NM 87545, Tel.: + (505)-667-0561; fax: + (505)-665-4292.

0032-3861/99/$ - see front matter
PII: S0032-3861(98)00826-X

Table 1
Pressing conditions and densities of composite films

Graphite content (vol.%)	Die pressure (psi)	Die temperature (°C)	Film density (actual/predicted) (g cm^{-3})
0	425	174–182	1.79/1.79
17	425	182–191	1.85/1.86
35	425	207–216	1.93/1.94
44	425	213–221	1.97/1.99
55	530	218–224	2.01/2.03
65	800	218–227	2.06/2.08

decrease its resistance to corrosion; the effect is even more pronounced if the voids are connected in a continuous network. In fabricating polymer/graphite composites, voids can potentially form within clusters of graphite particles or at graphite/polymer interfaces. In the case of interfacial voids, it is conceivable that if the graphite phase percolates as required for electrical conduction, a percolated void network could also form. Discrete voids, either at graphite–polymer interfaces or within graphite clusters, are less problematic.

Besides the presence of voids or void networks, the morphology of the polymeric component also influences the barrier properties of the composite material. In the case of a semicrystalline polymer, small molecules can diffuse only through amorphous regions. Thus if the presence of graphite alters the polymer crystallinity, barrier properties can be affected.

It is clear that the presence of graphite can significantly alter the barrier properties of CPC materials. The principal objective of this study is to characterize the effects of the presence and relative amount of graphite on the morphology (i.e. void content and crystallinity) of poly(vinylidene fluoride) (PVDF) composites and the concomitant effects of these morphological changes on barrier properties.

1.2. Sorption theory

One method of determining the void content of a CPC is to measure the sorption of a probe gas into the material. The void content of the composites studied here was interpreted within the framework of the so-called dual-mode sorption model, which is normally applied to glassy polymers. This model assumes that sorption occurs via two processes: (i) dissolution in the polymer (Henry's law absorption); and (ii) sorption into frozen-in ''holes'' or free volume in the glassy state (Langmuir adsorption). For rubbery polymers ($T > T_g$), only Henry's law mode sorption occurs, resulting in a linear sorption isotherm. In the glassy state ($T < T_g$), Henry's law sorption also occurs, but the presence of frozen-in free volume produces distinctive curvature in the isotherm, which is associated with a second mode of sorption termed the Langmuir mode. In the present case, the polymer is above its glass transition temperature, and we associate any Langmuir-mode sorption (isotherm curvature) with voids in the sample, either within graphite clusters or at polymer/graphite interfaces.

In the dual-mode model, the total concentration (C) of sorbed gas is obtained as the sum of the sorbed concentrations corresponding to each mode of sorption, viz.:

$$C = k_D P + \frac{C'_H b P}{(1 + bP)} \quad (2)$$

where k_D is the Henry's law constant, P is the gas pressure, C'_H is the Langmuir hole-filling capacity, and b is a hole affinity constant [9–11]. In this equation, the first term represents the Henry's law mode and the second represents the Langmuir mode of sorption. The parameter of particular interest here is the Langmuir capacity, C'_H, which can be taken as a measure of the pore volume in the composite samples [12]. The volume fraction of pores in the sample, f_p, can be calculated from:

$$f_p = (C'_H)(V_{ss})/(V_{STP}) \quad (3)$$

where V_{ss} (= 49 cc mol^{-1} for CO_2 [13,14]) is the sorbed-state molar volume of the penetrant and V_{STP} (= 22 400 cc mol^{-1}) is the penetrant molar volume at standard temperature and pressure. This sorption method for measuring porosity in polymers is very sensitive, provided that the probe gas has a low solubility (small k_D) in the bulk polymer. The method has been used successfully to quantify residual porosity and further gradual coalescence in polymeric latex films which were also above T_g [15,16].

2. Experimental

2.1. Sample preparation

A series of thin (∽130 μm) film samples was prepared from a commercial PVDF powder and a synthetic graphite which were dry-blended by ball milling. The PVDF powder is reported to have a molecular weight of 200–270 kg mol^{-1}, a polydispersity index ($\overline{M}_w/\overline{M}_n$) of 2.6 and a density of 1.785 g cm^{-3}. The graphite powder is reported to have a density of 2.24 g cm^{-3}, and is specified to have 99% of particles pass through a 200 mesh (75 μm opening) sieve, and 80%–90% pass through a 325 mesh (44 μm opening) sieve. Films were consolidated in a Carver laboratory press with heated platens using a mold specifically designed to produce films of known and uniform thickness. Pressing conditions were varied according to the graphite content of the mixed powders, but in each case pressure was maintained while the mold was heated to the desired temperature, held for 10 min, then air cooled to room temperature. To check consolidation quality, the densities of the pressed films were measured using a conventional Archimedes technique. Pressing conditions for the films, along with their measured and predicted densities, are provided in Table 1.

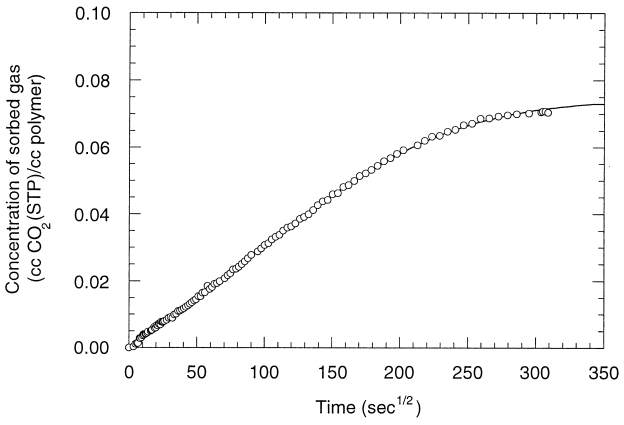

Fig. 1. Sorption kinetics curve for CO_2 at 93 Torr in a 44 vol.% graphite sample at 30°C. The solid line represents a fit to the data using Eq. 4.

2.2. Sorption and diffusion experiments

Sorption experiments using CO_2 as a probe gas were performed to identify the barrier characteristics of the composites, including the presence and connectivity of voids. CO_2 was chosen as the probe gas due to its inertness and low solubility in PVDF. With a low penetrant solubility in the bulk polymer, sorption by voids dominates the overall sorption level, and the dual-mode sorption model can be used to accurately determine pore volume.

Sorption data were collected by a conventional gravimetric method using a computer-interfaced Cahn C-2000 electrobalance. The chamber containing the sample was evacuated and the sample was degassed until the sample weight stabilized. The chamber was then backfilled with CO_2 to the desired pressure, and the weight gain of the sample was monitored as a function of time. Once equilibrium was reached, additional CO_2 was introduced into the sample chamber to reach the next desired pressure and the data collection process was repeated. Data for 30°C sorption isotherms were collected in this manner through successive sorption runs at increasing CO_2 pressures, without re-evacuating or removing the sample from the chamber between runs.

Each sorption run produces a single sorption kinetics curve. Sorption kinetics curves are typically plotted as the amount of penetrant sorbed (M_t) at a fixed temperature and pressure versus the square root of sorption time [17], as depicted in Fig. 1. This allows convenient use of:

$$\frac{M_t}{M_\infty} = \phi(y)f(y) + [1 - \phi(y)]g(y) \tag{4}$$

which is an approximation developed by Balik [18] to describe Fickian diffusion in a thin film of thickness ℓ. In Eq. 4, $y = Dt/\ell^2$, $f(y) = 4(y/\pi)^{1/2}$, $g(y) = 1 - (8/\pi^2)\exp(-\pi^2 y)$, and $\phi(y)$ is a weighting function. From each curve, a diffusion coefficient (D) and an equilibrium sorption level (M_∞) are obtained by fitting Eq. 4 to the sorption data. Sorption isotherms are then obtained by plotting the cumulative values of M_∞, adjusted for the polymer content of the composite as a function of penetrant pressure.

2.3. Differential scanning calorimetry

A DuPont 9900 differential scanning calorimeter was used to obtain thermograms at heating and cooling rates of 20°C min^{-1} for all the specimens. The heat of fusion obtained from the first scan was used to calculate the degree of crystallinity for the as-molded samples. After melting, samples were held at 300°C for 2 min, then were cooled at 20°C min^{-1} to determine the crystallization temperature. Melting temperatures, crystallization temperatures and heats of fusion were recorded for each sample.

2.4. Scanning electron microscopy

Smooth cross-sections for microscopic observation were obtained by sectioning the composite samples in a Reichert–Jung Ultracut S cryo-ultramicrotome. Sectioning was performed at −100°C to avoid deformation of the samples which would result if they were sectioned above −30°C, the glass transition temperature of PVDF, as determined by differential scanning calorimetry. The microtomed cross-sections of the samples were imaged using a Hitachi S-3200N environmental scanning electron microscope operated at 15–30 kV. Since no conductive coating was applied, specimen charging was eliminated by operating the microscope at a partial pressure of 15–20 Pa. Images were collected from backscattered electrons, providing atomic number contrast between the fluorinated polymer and graphite as a means of discriminating the two components.

2.5. Electrical conductivity measurements

Measurements of electrical conductivity were used to determine the graphite percolation threshold of this PVDF/graphite system. Bulk electrical resistivities of the composite samples were measured using a standard four-point probe device. This instrument applies a constant current (I) to the sample through two of the probes, and the resulting voltage (V) across the other two is measured. For a sample of finite thickness, w, the resistivity (ρ) is calculated as:

$$\rho = (V/I)wCF \tag{5}$$

where C and F are geometric correction factors for sample width/diameter and thickness, respectively [19]. The limiting value of C is $\pi/\ln 2 = 4.532$ for samples whose width and length (in the case of rectangular samples) or diameter (in the case of circular samples) are many times greater than the probe spacing (s). The value of F approaches unity as w/s approaches zero. Exact values of C and F for specific test geometries may be calculated or read from tables such as those provided in Smits [19]. Alternatively, many four-point probe devices calculate one or both of the correction factors internally. In the present case, the appropriate values

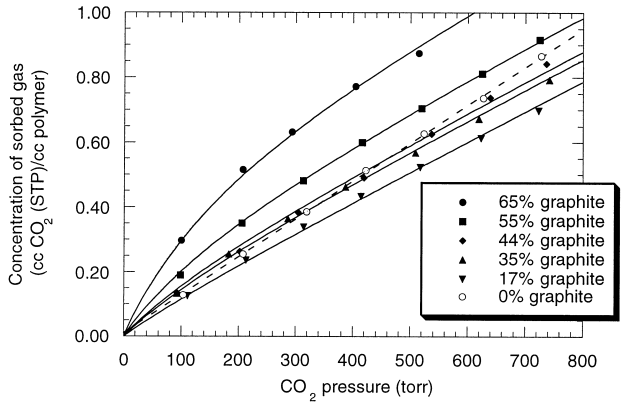

Fig. 2. Sorption isotherms for CO_2 in six PVDF/graphite composites at 30°C. Pure PVDF (0 vol.% graphite) exhibits Henry's law behavior, as shown by the linear fit (dashed line). The isotherms for the graphite-containing samples all exhibit curvature, indicating that some porosity is present. Solid lines are fits to the dual-mode sorption model (Eq. 2).

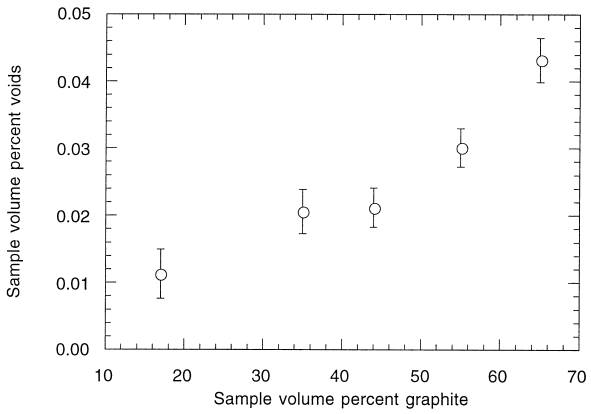

Fig. 3. Composition dependence of composite void content.

of C were automatically applied to Eq. 4 by the instrument; the samples were sufficiently thin relative to the probe spacing so that no thickness correction was needed ($F = 1$). Values of bulk electrical conductivity, $\sum$, were obtained by simply inverting the corresponding values of resistivity, ρ.

3. Results and discussion

3.1. Sorption and diffusion results

Sorption isotherms acquired at 30°C for CO_2 in the five composite films and a pure PVDF film are shown in Fig. 2. Data are normalized for the amount of polymer in each sample. The pure PVDF film exhibited Henry's law behavior, as expected for a polymer above its glass transition temperature (T_g). Sorption isotherms for the composite films possessed distinctive curvature reminiscent of a glassy polymer, even though the polymer component was well above T_g. These isotherms could be quantitatively described by the dual-mode sorption model given in Eq. 2.

A computer program incorporating the Levenberg–Marquardt nonlinear regression algorithm was used to simultaneously fit Eq. 2 to all five experimental isotherms for the composite samples using single values of k_D and b, and five different values of C'_H. This choice was based on minimizing the number of adjustable parameters and taking into account the similarities among the various samples. The pure PVDF sample was allowed to have a different value of k_D than the composites to account for morphological differences due to the absence of graphite (see the DSC results later). The dual-mode parameters obtained from the nonlinear regression, along with the corresponding void fractions, are listed in Table 2.

The void fractions in Table 2 were calculated from the C'_H values using Eq. 3. These numbers have been adjusted for the amount of polymer in each sample to yield void volume fractions on a total sample volume basis. As expected, the pure PVDF sample contained no voids (no isotherm curvature), but the composite samples possessed void fractions that increased with increasing graphite loading level, suggesting that the voids may be associated with incomplete wetting at polymer/graphite interfaces. This composition dependence of void content is illustrated in Fig. 3. From Fig. 2, it is evident that the voids have a large effect on the sorption behavior of the composites, even though the void fractions are very small. The magnitude of the void fractions also illustrates the degree of sensitivity of this technique for detecting the presence of voids. The minute volume of voids present also suggests that a connected network of voids is highly unlikely.

Table 2
Dual-mode parameters

Graphite content (vol.%)	k_D[a] (×10^4)	b[b] (×10^3)	C'_H[c]	Sample void fraction (×10^4)
0	11.92 ± 0.05	–	–	–
17	9.19 ± 0.25	5.84 ± 0.93	0.062 ± 0.020	1.13 ± 0.36
35	9.19 ± 0.25	5.84 ± 0.93	0.144 ± 0.023	2.06 ± 0.33
44	9.19 ± 0.25	5.84 ± 0.93	0.174 ± 0.024	2.17 ± 0.29
55	9.19 ± 0.25	5.84 ± 0.93	0.302 ± 0.029	3.01 ± 0.29
65	9.19 ± 0.25	5.84 ± 0.93	0.564 ± 0.043	4.32 ± 0.33

[a] k_D = [cc CO_2(STP)/cc polymer-Torr].
[b] b = [Torr^{-1}].
[c] C'_H = [cc CO_2(STP)/cc polymer].

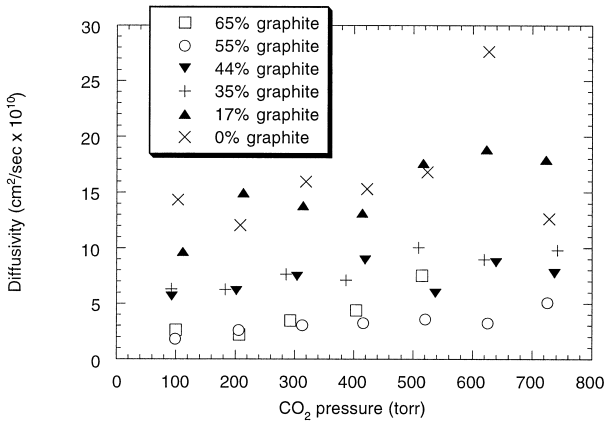

Fig. 4. Diffusivities (D) of CO_2 in six PVDF/graphite composites as a function of CO_2 pressure.

CO_2 diffusion coefficients (D) obtained from plots such as Fig. 1 at each pressure are displayed as a function of penetrant pressure in Fig. 4 for all of the samples. The CO_2 diffusivities are essentially independent of pressure. To determine the effect of graphite loading level on D, a mean diffusivity ($< D >$) for each sample was calculated from the set of values at each CO_2 pressure. The unusually high diffusivity for CO_2 in the pure PVDF sample at 627 Torr was omitted in calculating $< D >$ for that sample. The mean diffusivities of the samples are plotted as a function of graphite content in Fig. 5.

Although it is somewhat evident from Fig. 4, Fig. 5 clearly shows that above 17 vol.% graphite, diffusivity decreases with increasing graphite content. This was the expected trend, since the graphite was assumed to be impenetrable by the CO_2 and exhibited no measurable CO_2 uptake in sorption studies conducted with pure graphite powder. Graphite in sufficient concentrations therefore appears to serve as a barrier to diffusion by creating a more tortuous path for diffusing penetrant molecules. A connected void network would create an open diffusive pathway for CO_2 molecules, and would

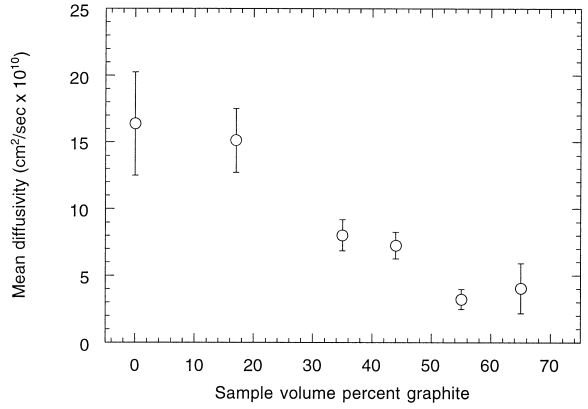

Fig. 5. Composition dependence of the mean diffusivity ($< D >$) of CO_2 in six PVDF/graphite composites.

presumably cause an increase in CO_2 diffusivity. The decrease in $< D >$ with increasing graphite content indicates that the voids are not connected in a continuous network.

3.2. Morphological characterization

Environmental SEM was used to qualitatively characterize the distribution of graphite particles within the PVDF matrix. Cross-sectional images showed no evidence of a preferred orientation of graphite particles. Although there appear to be several small clumps of graphite particles, the graphite is generally well-dispersed. A typical environmental SEM micrograph of a composite sample containing 55 vol.% graphite is provided in Fig. 6.

The crystallinity of the polymer portions of the samples was characterized by differential scanning calorimetry (DSC). The primary objective of the DSC analysis was to determine differences in nucleation behavior and degree of crystallinity between the PVDF and composite samples. Although morphological differences here are primarily attributed to the presence of graphite, note that the samples did have slightly different thermal histories due to differences in their molding temperatures (see Table 1). The DSC cooling profiles are displayed in Fig. 7. Crystallization temperatures for samples containing graphite are consistently several degrees higher than that of the neat polymer, which strongly suggests that graphite particles act as heterogeneous nucleation sites for PVDF crystals. Crystallization temperatures and other quantities obtained from DSC analysis are listed in Table 3. The heats of fusion (ΔH_f) listed in the table are the integrated areas of the melting endotherms between 150 and 195°C. Degrees of crystallinity were calculated based on a value of $\Delta H_f = 105\ J\ g^{-1}$ for 100% crystalline PVDF [20].

With the exception of the 65 vol.% graphite sample, the heats of fusion of the PVDF in graphite-containing samples are consistently higher than that of the pure polymer, indicating that the PVDF in the composite samples has a higher degree of crystallinity than the neat PVDF. Since sorption of CO_2 does not occur in crystalline polymer regions, the increase in PVDF crystallinity associated with the presence of graphite corresponds to the lower Henry's law constant (k_D) obtained for samples containing graphite (see Table 2). Melting temperatures for PVDF are also slightly higher in the presence of graphite, which suggests that the lamellar polymer crystals may be somewhat thicker in the composite samples than in the pure PVDF.

Since there is no evidence from the sorption experiments that pure PVDF samples contain voids, it follows that voids are somehow associated with the presence of graphite. Given the above evidence that PVDF nucleates heterogeneously on graphite particles, a possible mechanism for void formation is poor particle wetting. Crystallization results in a densification of the polymer molecules, so shrinkage along graphite interfaces may accompany crystallization and

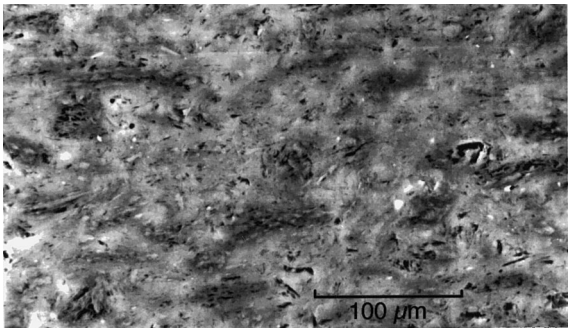

Fig. 6. A PVDF/graphite composite containing 55 vol.% graphite which has been cryo-microtomed and imaged in an environmental SEM at a pressure of 15–20 Pa. Backscattered electrons are utilized to provide atomic number contrast between fluorine (polymer phase, light) and carbon (graphite phase, dark).

result in particle dewetting. Another possibility is that voids exist within clumps of graphite particles. SEM provides evidence of some graphite clumps, but whether the clumps contain voids is unknown.

Regardless of their location, the voids in these CPCs have an important effect on the barrier properties of PVDF containing graphite, but there is an apparent trade-off between porosity and crystallinity effects. In samples with low graphite concentrations, decreased sorptive capacity due to increased PVDF crystallinity seems to outweigh the increase in sorptive capacity due to the presence of voids (see Fig. 2). For samples with high graphite loading, the opposite holds true.

3.3. Determination of the graphite percolation threshold

The measured bulk electrical conductivities of the composite samples are plotted in Fig. 8 as a function of graphite content. Two theoretical fits of Eq. 1 also appear in the figure. One curve fit (Fit 1) allows both the percolation threshold, p_c, and the exponent, μ, to float during regression. In the other fit (Fit 2), μ is set to a fixed value of 2 (the theoretical value for three-dimensional systems [8]) so that only p_c is calculated. These two approaches produce nearly identical results, as represented by the solid and dotted lines in Fig. 8. According to Fit 1, the regressed value of μ was 2.14 ± 0.04, which lies within 10% of the hypothetical value of 2. Since a very low but measurable conductivity was achieved in the 35% graphite sample but no conductivity was detected for the 17% graphite sample, the percolation threshold was anticipated to lie between these two values. The diffusion coefficient data in Fig. 5 also suggest a percolation threshold between 0.17 and 0.35; while a 17% graphite loading has little effect on $< D >$, a significant decrease in D occurs at a loading of 35%. Indeed, the calculated percolation thresholds for Fit 1 and Fit 2 were in close agreement with prediction and each other, with $p_c = 0.319 \pm 0.004$ for Fit 1 and $p_c = 0.333 \pm 0.002$ for Fit 2. With this evidence, it seems reasonable to expect graphite percolation to first occur at loadings of 31–34 vol.% in this PVDF-matrix system.

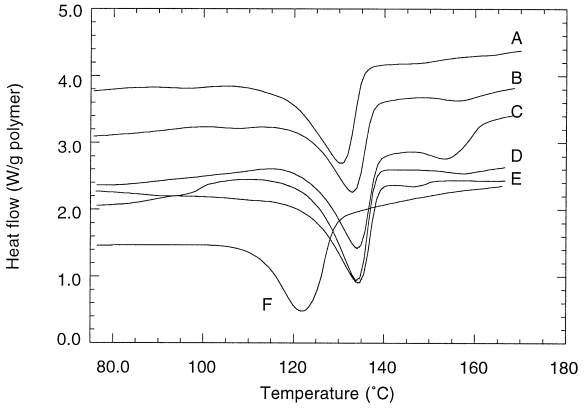

Fig. 7. DSC cooling (crystallization) profiles for six samples. A = 17 vol.% graphite; B = 44 vol.% graphite; C = 65 vol.% graphite; D = 35 vol.% graphite; E = 55 vol.% graphite; F = pure PVDF.

4. Conclusions

Graphite acts as a barrier to the sorption and diffusion of CO_2 in PVDF. A percolated graphite network, present at graphite concentrations greater than 31–34 vol.%, creates a more tortuous path for diffusing probe-gas molecules such as CO_2, resulting in decreasing CO_2 diffusivity with increasing graphite content. The presence of graphite particles also induces heterogeneous nucleation and increased crystallinity of PVDF. Small amounts of voids are present, but are not percolated, in graphite/PVDF composite samples, and the volume fraction of voids increases with increasing graphite content. Given this trend and that PVDF nucleates heterogeneously on graphite particles, the most likely mechanism for void formation in these composite materials is poor particle wetting. The densification that accompanies polymer crystallization may result in shrinkage along graphite interfaces and subsequent particle dewetting. Both increased PVDF crystallinity and the presence of voids contribute to the sorptive characteristics

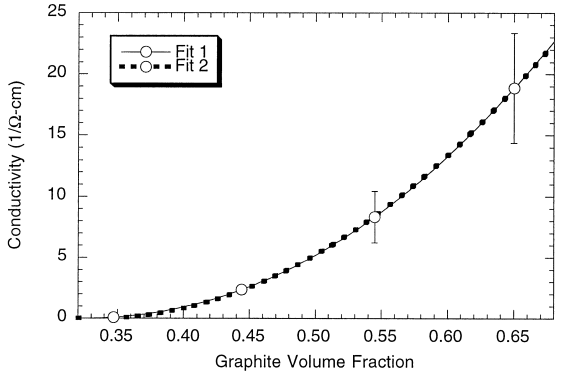

Fig. 8. Electrical conductivities of graphite/PVDF composite films. Open circles = data; solid and dotted lines = fits to Eq. 1 (see text).

Table 3
Results of differential scanning calorimetry

Graphite content (vol.%)	ΔH_f (J g^{-1} polymer)	Crystallinity (%)	T_{melt} (onset, °C)	T_{cryst} (onset, °C)
0	38.0	36.1	163	129
17	42.7	40.6	164	135
35	41.3	39.3	164	138
44	39.2	37.3	165	137
55	41.2	39.2	164	138
65	36.4	34.7	164	138

of the composites. At low graphite loading levels, crystallinity effects dominate, resulting in decreased sorptive capacity relative to pure PVDF. In samples with high graphite loading, the opposite holds true, as higher void fractions result in greater sorptive capacity.

Acknowledgements

The authors thank Mickey Gregory, Thomas Malow, Drew Hanser and Changhe Bai for their assistance with various instrumentation and Tom Hare for performing the nonlinear dual-mode regressions.

References

[1] Lawrance RL. US patent no. 4214969, 1980.
[2] Ezquerra TA, Kulescza M, Balta-Calleja FJ. Synth Metals 1991;41:915.
[3] Navarro J, Roig A, Noguera P, Vicente F, Vilaplana J, López J. J Mater Sci 1994;29:4604.
[4] Blaszkiewicz M, McLachlan DS, Newnham RE. Polym Eng Sci 1992;32:421.
[5] Martinez-Salazar J, Bayer RK, Ezquerra TA, Balta-Calleja FJ. Colloid Polym Sci 1989;267:409.
[6] Wang J, Martinez T, Yaniv DR, McCormick L. J Electroan Chem Interfacial Electrochem 1990;286:265.
[7] Viswanathan R, Heaney MB. Phys Rev Lett 1995;75:4433.
[8] Stauffer D. Introduction to percolation theory. Philadelphia: Taylor and Francis, 1985.
[9] Barrer RM, Barrie JA, Slater J. J Polym Sci 1958;27:177.
[10] Michaels A, Vieth W, Barrie J. J Appl Polym Sci 1963;34:1.
[11] Vieth WR, Sladek K. J Colloid Sci 1965;20:10.
[12] Gregg SL, Sing KSW. Adsorption, surface area and porosity. 2nd ed. New York: Academic, 1982.
[13] Koros WJ, Paul DR. J Polym Sci Polym Phys Ed 1978;16:1947.
[14] Kirchheim R. J Polym Sci B Polym Phys 1993;31:1373.
[15] Balik CM, Said MA, Hare TM. J Appl Polym Sci 1989;38:557.
[16] Balik CM, Said MA. Proc MRS 1990;215:199.
[17] Rogers CE. In: Fox D, editor. Physics and chemistry of the organic solid state, vol. 1. New York: Interscience, 1963, chap. 6.
[18] Balik CM. Macromolecules 1996;29:3025.
[19] Smits FM. Bell Syst Tech J 1958;37:711.
[20] Nakagawa K, Ishida Y. J Polym Sci Polym Phys Ed 1973;11:2153.